The following Communications have been judged by at least two referees to be "very important papers" and will be published online at www.angewandte.org soon:

*H. Herrmann, J. L. Fillol, H. Wadepohl, L. H. Gade**
Atom-by-Atom Assembly of EN_2^{2-} Units (E=S, Se) by Chalcogen Atom Transfer in the Coordination Sphere of a Transition Metal

*J.-E. Lee, J. Yun**
Catalytic Asymmetric Boration of Acyclic α,β-Unsaturated Esters and Nitriles

S.-T. Wu, Y.-R. Wu, Q.-Q. Kang, H. Zhang, L.-S. Long, Z. Zheng,* R.-B. Huang, L.-S. Zheng*
Chiral Symmetry Breaking by Chemically Manipulating Statistical Fluctuation in Crystallization

*F. Arnesano, S. Scintilla, G. Natile**
Interaction between Platinum Complexes and a Methionine Motif Found in Copper Transport Proteins

*F. Akagi, T. Matsuo, H. Kawaguchi**
Dinitrogen Cleavage by a Diniobium Tetrahydride Complex: Formation of a Nitride and Its Conversion to Imide Species

J.-H. Jang, D. Dendukuri, T. A. Hatton, E. L. Thomas, P. S. Doyle**
A Route to Three-Dimensional Structures in a Microfluidic Device: Stop-Flow Interference Lithography

Books

Highlights

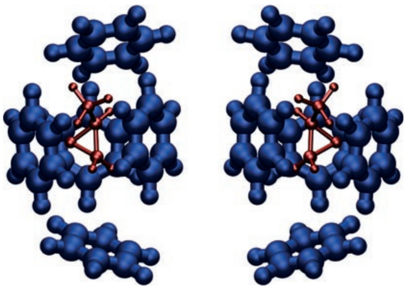

The solvent makes the difference: Quantum chemical investigations show that chiroptical properties can originate mainly from a chiral solvent shell rather than from the chiral solute. By using this approach it is possible to explain, for example, why the optical rotation of (*S*)-methyloxirane is positive in water, but has a relatively strong negative value in benzene (see picture; red: (*S*)- or (*R*)-methyloxirane, blue benzene).

Induced Chirality

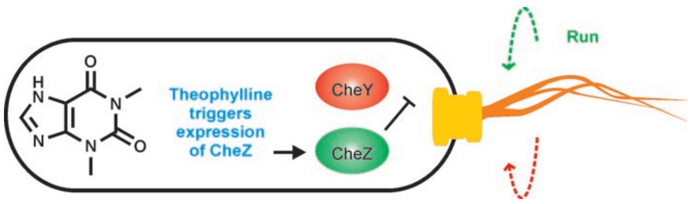

A demanding challenge for the genetic modification of organisms that could target pollutants or diseases in future applications will be the recruitment of such entities to the respective sites of action. Topp and Gallivan have used RNA switches to guide bacteria along paths of specific compounds by rewiring their chemosensory system (see picture; the CheZ protein controls the motility).

RNA Technologies

Contents

Reviews

H/D Exchange

A favorable exchange: Deuterated organic compounds may be prepared significantly more efficiently and more cost effectively by H/D exchange rather than by classical synthetic procedures. In this Review, the development of methods for the preparative application of the H/D-exchange reaction on a carbon center (see picture) over the last ten years are brought together and discussed.

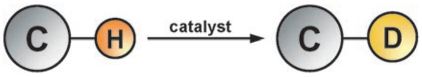

Communications

Protein Structures

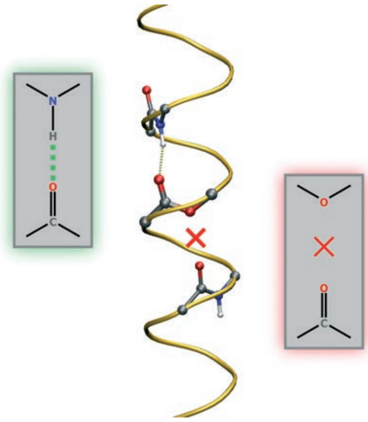

The latest twist: The effect of backbone H-bonding on the stability of proteins was studied by experimental techniques and molecular dynamics simulation. The structure of the coiled-coil model peptide examined (see picture) is affected by interactions in the solvent-exposed regions as well as by interhelical hydrophobic interactions.

Water Splitting

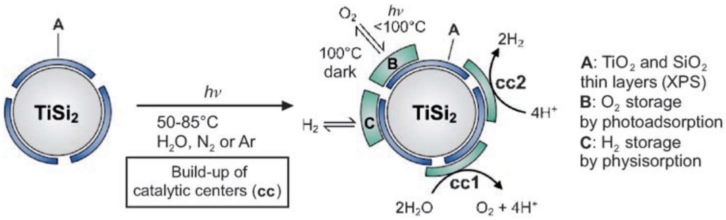

Divide and separate: Photocatalytic splitting of water into hydrogen and oxygen is achieved with a catalyst which is formed on the surface of titanium dicilicide (see picture). The two product gases are reversibly physisorbed by the catalyst. Desorption of hydrogen occurs at ambient temperature, but oxygen is entirely stored up to 100 °C in light and can be released upon heating at this temperature in the dark, which allows convenient separation of the gases.

For the USA and Canada:
ANGEWANDTE CHEMIE International Edition (ISSN 1433-7851) is published weekly by Wiley-VCH, PO Box 191161, 69451 Weinheim, Germany. Air freight and mailing in the USA by Publications Expediting Inc., 200 Meacham Ave., Elmont, NY 11003. Periodicals postage paid at Jamaica, NY 11431. US POSTMASTER: send address changes to *Angewandte Chemie*, Wiley-VCH, 111 River Street, Hoboken, NJ 07030. Annual subscription price for institutions: US$ 5685/5168 (valid for print and electronic / print or electronic delivery); for individuals who are personal members of a national chemical society prices are available on request. Postage and handling charges included. All prices are subject to local VAT/ sales tax.

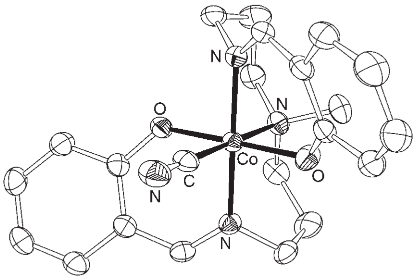

Canning a carbon: During oxidation with O_2, the cobalt(II) complex [Co(salmdpt)] (salmdptH_2 = bis[3-(salicylideneimino)-propyl]methylamine) reacts with a nitrile substrate to form the cyanide complex [Co(salmdpt)CN] (see structure) and the corresponding aldehyde, which contains one less carbon atom than the starting nitrile.

Cobalt Complexes

J. Müller, C. Würtele, O. Walter,
S. Schindler* ________ **7775 – 7777**

Transformation of Nitrile to Cyanide and Aldehyde Using a Cobalt(II) Complex and Dioxygen

---

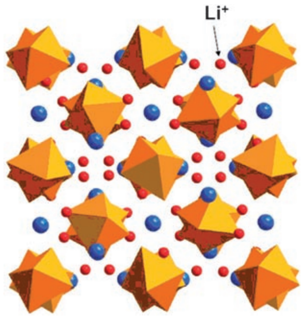

Low activation energy and fast lithium ion conduction have been observed for the new compound $Li_7La_3Zr_2O_{12}$. Relative to previously reported lithium garnets, the solid electrolyte shows a larger cubic lattice constant, higher lithium ion concentration, lower degree of chemical interaction between the Li^+ ions and the other lattice constituents, and higher densification.

Lithium Batteries

R. Murugan,* V. Thangadurai,
W. Weppner* ________ **7778 – 7781**

Fast Lithium Ion Conduction in Garnet-Type $Li_7La_3Zr_2O_{12}$

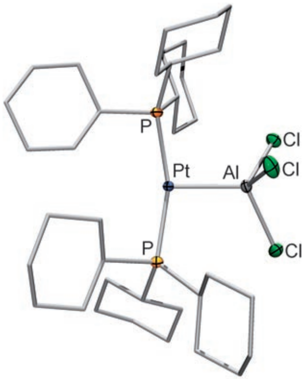

You'll never walk alane: An intriguing T-shaped platinum–alane adduct results from the almost quantitive reaction of $[Pt(PCy_3)_2]$ with AlX_3 (X = Cl, Br, I). The compound $[(Cy_3P)_2Pt{-}AlCl_3]$ represents the first neutral alane complex displaying an unsupported Pt–Al dative bond.

Platinum Complexes

H. Braunschweig,* K. Gruss,
K. Radacki ________ **7782 – 7784**

Interaction between d- and p-Block Metals: Synthesis and Structure of Platinum–Alane Adducts

---

Without π stabilization: Phosphine-induced cleavage of a dinuclear precursor yielded the first terminal alkylborylene complex. Experimental and computational data suggest a strong Mn–B interaction, thus compensating the lack of π stabilization provided by the B-bound alkyl group and accounting for the thermal stability of the title compound and its propensity to undergo controlled derivatization.

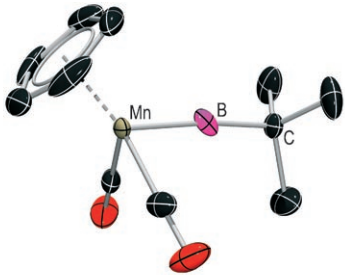

Borylene Complexes

H. Braunschweig,* M. Burzler, T. Kupfer,
K. Radacki, F. Seeler ________ **7785 – 7787**

Synthesis and Electronic Structure of a Terminal Alkylborylene Complex

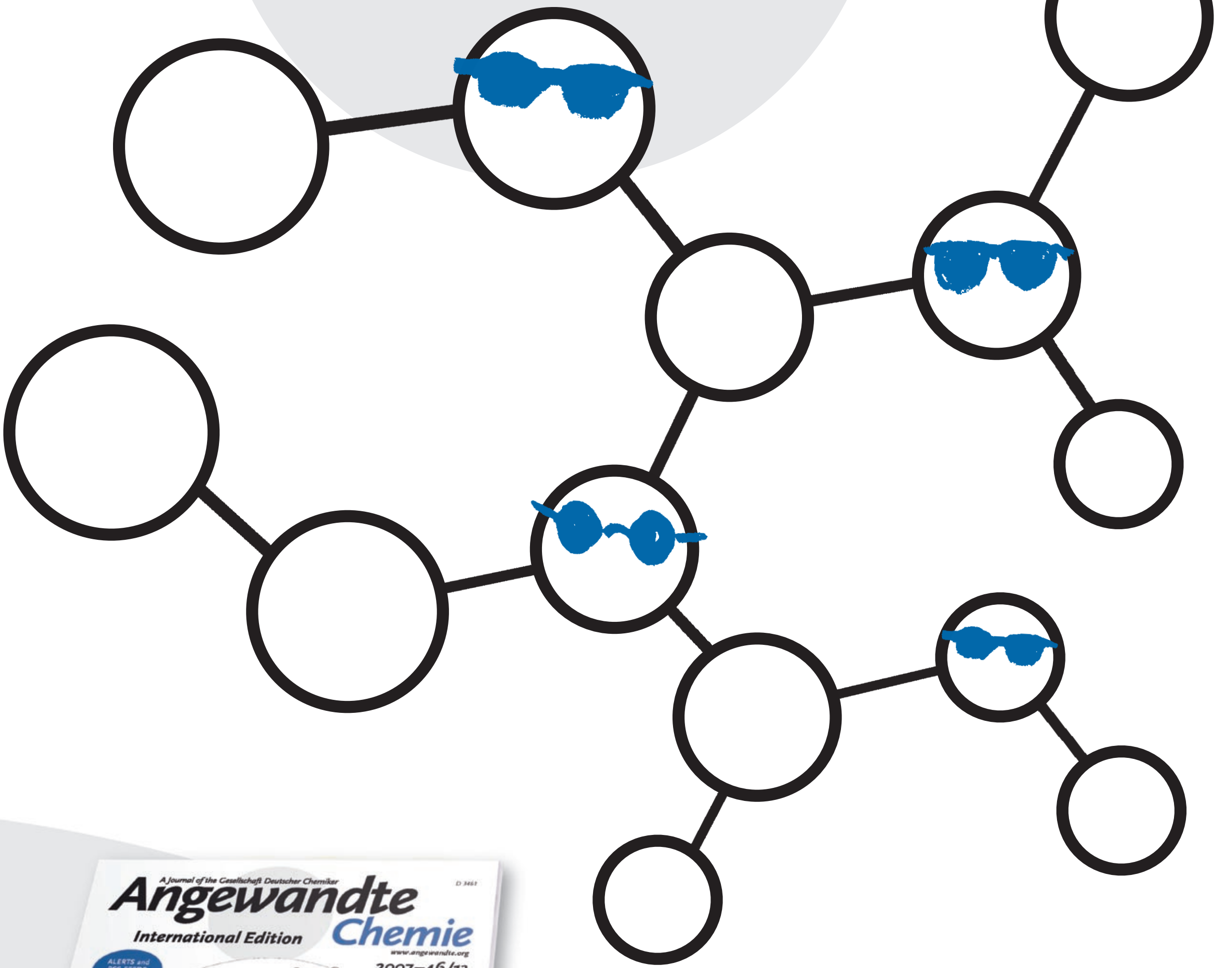

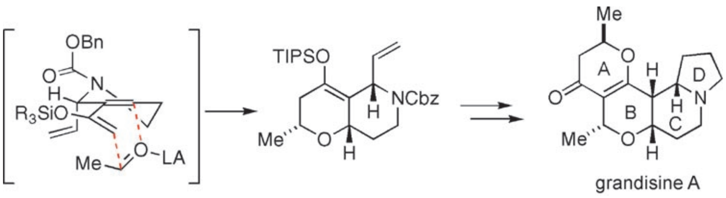

Controlled fusion: The use of a seco ring D precursor to control both the stereochemistry of a critical cycloaddition with acetaldehyde and the direction of protonation of the resultant silyl enol ether cycloadduct has led to the total synthesis of grandisine A, which shows promising selectivity for binding to the δ-opioid receptor. The D ring is installed in the final stages of the synthesis (see scheme, LA = Lewis acid).

Natural Products

D. J. Maloney,
S. J. Danishefsky* ———— 7789–7792

Conformational Locking through Allylic Strain as a Device for Stereocontrol—Total Synthesis of Grandisine A

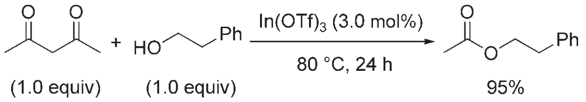

Retro-aldol reaction: Indium-catalyzed reaction of a 1,3-diketone with an alcohol proceeds under solvent-free conditions by nucleophilic attack of the alcohol on a carbonyl group of the 1,3-diketone and carbon–carbon bond cleavage by a retro-Claisen condensation to give an ester in high yield (see scheme). Using water and an amine as nucleophiles instead of an alcohol gave the corresponding carboxylic acid and amide.

Synthetic Methods

A. Kawata, K. Takata, Y. Kuninobu,*
K. Takai* ———— 7793–7795

Indium-Catalyzed Retro-Claisen Condensation

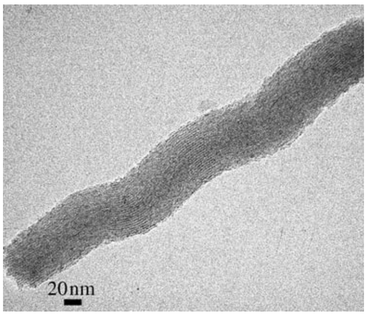

Keep this handy! Periodic mesoporous organosilica-based compounds with chiral channels are prepared by using an achiral fluorinated surfactant (FC-4911) and cetyltrimethylammonium bromide as structure-directing agents. Spiral samples synthesized from 1,4-bis(triethoxysilyl)benzene exhibit structural periodicity and a crystal-like mesoporous wall (see TEM image).

Mesoporous Materials

X. Meng, T. Yokoi, D. Lu,
T. Tatsumi* ———— 7796–7798

Synthesis and Characterization of Chiral Periodic Mesoporous Organosilicas

Any substituent does it: The hydroboration of vinyl arenes with pinacol borane (HBPin) and cationic rhodium complexes selectively placed the boron proximal to the aryl rather than phenyl ring, regardless of whether this ring bears electron-donating or electron-withdrawing substituents. In competition experiments between styrene and various vinyl arenes, preferential hydroboration also occured at the substituted arene (see scheme). Hammett plots indicate a break in the mechanism.

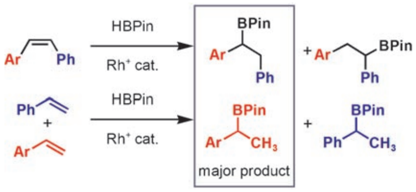

Metal-Catalyzed Hydroborations

D. R. Edwards, Y. B. Hleba, C. J. Lata,
L. A. Calhoun,
C. M. Crudden* ———— 7799–7802

Regioselectivity of the Rhodium-Catalyzed Hydroboration of Vinyl Arenes: Electronic Twists and Mechanistic Shifts

Asymmetric Catalysis

F. Berthiol, R. Matsubara, N. Kawai, S. Kobayashi* ______ **7803 – 7805**

Catalytic Asymmetric Michael Reactions with Enamides as Nucleophiles

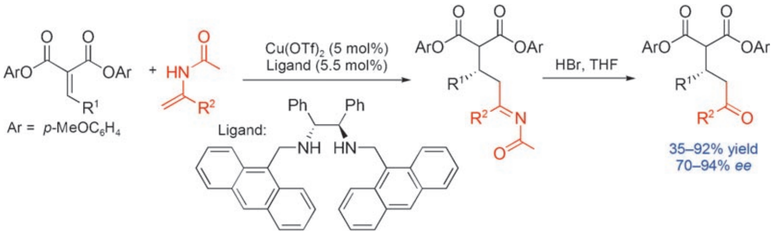

Under its own steam: No external proton source is required for catalytic turnover in the copper-catalyzed title reaction with alkylidenemalonates, as proton transfer occurs rapidly in an intramolecular manner. The desired 1,5-dicarbonyl adducts were formed in moderate to high yield with high enantioselectivity (see scheme). R^1 = alkyl; R^2 = alkyl, aryl; Tf = trifluoromethanesulfonyl.

Asymmetric Catalysis

T. E. Reynolds, K. A. Scheidt* ______ **7806 – 7809**

Catalytic Enantioselective α-Acylvinyl Anion Reactions of Silyloxyallenes

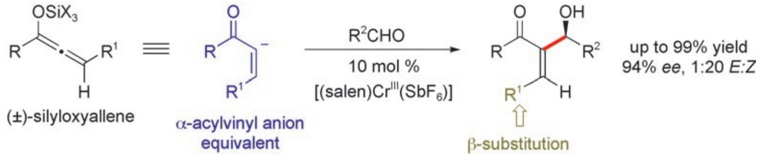

Alternatives with silicon: The enantioselective Lewis acid catalyzed addition of racemic silyloxyallenes to aldehydes is reported. A {(salen)Cr^{III}} complex efficiently catalyzes the reaction of these α-acylvinyl anion equivalents (see scheme) with excellent enantioselectivity, high yield, and superb control over the configuration of the resulting double bond.

Asymmetric Catalysis

D.-Y. Wang, X.-P. Hu,* J.-D. Huang, J. Deng, S.-B. Yu, Z.-C. Duan, X.-F. Xu, Z. Zheng* ______ **7810 – 7813**

Highly Enantioselective Synthesis of α-Hydroxy Phosphonic Acid Derivatives by Rh-Catalyzed Asymmetric Hydrogenation with Phosphine–Phosphoramidite Ligands

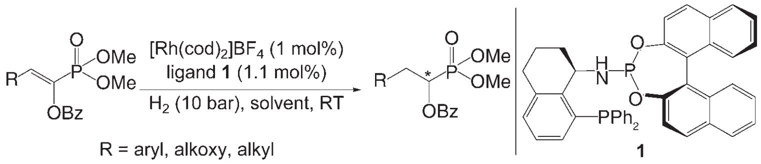

A class act: Unsymmetrical hybrid phosphine–phosphoramidite ligands with central and axial chirality are applied to the highly enantioselective hydrogenation of various enol ester phosphonates (see scheme; cod = cycloocta-1,5-diene). Enantioselectivities up to 99.9 % *ee* are obtained for all classes of β-aryl, β-alkoxy, and β-alkyl substrates.

Gold Ethylene Complexes

H. V. R. Dias,* J. Wu ______ **7814 – 7816**

Thermally Stable Gold(I) Ethylene Adducts: $[(HB\{3,5\text{-}(CF_3)_2Pz\}_3)Au(CH_2{=}CH_2)]$ and $[(HB\{3\text{-}(CF_3),5\text{-}(Ph)Pz\}_3)Au(CH_2{=}CH_2)]$

Captured by scorpionates: Using fluorinated scorpionates, remarkably stable gold(I) complexes containing ethylene are isolated and structurally characterized (see structure of molecule core: yellow Au, blue N, red B, light gray C). These adducts feature κ^2-bonded tris(pyrazolyl)borate ligands, and show in the ^{1}H and ^{13}C NMR spectra considerably upfield-shifted ethylene signals.

Phytopathogens

L. A. Paquette,* X. Peng,
J. Yang **7817 – 7819**

Asymmetric Synthesis of the Phytopathogen (+)-Fomannosin

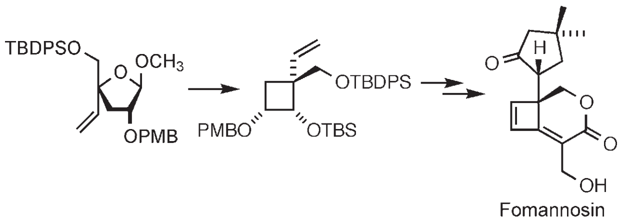

Three new construction features in one synthesis—for the fused cyclobutene ring, the cyclopentanone, and the functionalized six-membered lactone—characterize the procedure that leads to the natural (+)-enantiomer of the title compound starting with D-glucose. Central to the routing are steps involving organometallic reagents containing ruthenium, osmium, zirconium, and samarium among others.

Gold Catalysts

A. Corma,* C. González-Arellano,
M. Iglesias, F. Sánchez **7820 – 7822**

Gold Nanoparticles and Gold(III) Complexes as General and Selective Hydrosilylation Catalysts

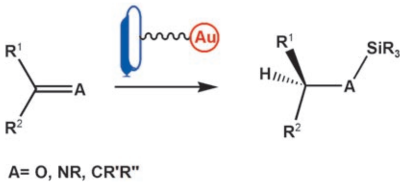

Worth their weight in gold: Au/CeO_2 nanoparticles are a highly active catalyst for the hydrosilylation of a large variety of unsaturated compounds with high chemo- and regioselectivity. To understand the nature of the catalytic active sites, Au^I and Au^{III} phosphine-free stable organogold complexes and their supported counterparts were prepared and their relative activity towards hydrosilylation was elucidated.

Arene Interactions

W. B. Motherwell,* J. Moïse, A. E. Aliev,*
M. Nič, S. J. Coles, P. N. Horton,
M. B. Hursthouse, G. Chessari,
C. A. Hunter, J. G. Vinter **7823 – 7826**

Noncovalent Functional-Group–Arene Interactions

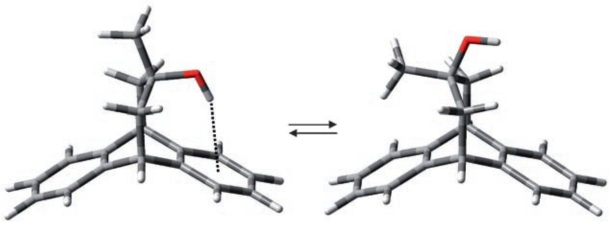

Hanging in the balance: A series of dibenzobicyclo[3,2,2]nonanes provides a delicate conformational balance for investigating weak interactions, such as O−H⋯π(Ar) π-hydrogen bonding (see scheme, red O) and solvent–solute interactions. The models are designed to probe the effectiveness of replacing a hydroxy group by fluorine or to compare the arene affinities of sulfur and oxygen.

Antimony Compounds

F. García, R. J. Less, V. Naseri,
M. McPartlin, J. M. Rawson,*
D. S. Wright* **7827 – 7830**

Formation and Structure of the $[(1,2\text{-}C_6H_4P_2Sb)_2]^{4-}$ Ion: Implications for an Extended Family of Isoelectronic Main-Group Radicals

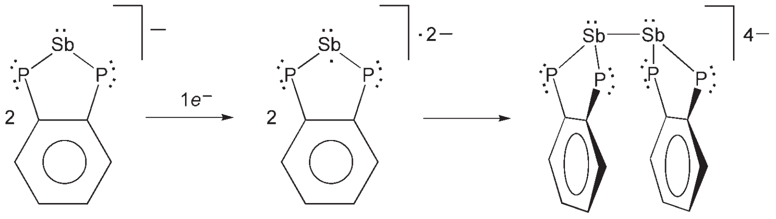

A fine pair: Quadruple deprotonation of $1,2\text{-}(PH_2)_2C_6H_4$ with $Sb(NMe_2)_3$/nBuLi gives the 6π-aromatic ion $[1,2\text{-}C_6H_4P_2Sb]^-$, which is converted by one-electron reduction into the radical $[1,2\text{-}C_6H_4P_2Sb]^{\bullet 2-}$ (see picture). DFT calculations reveal that dimerization of the radical is only favored if ionic interactions with cations are considered.

Natural Product Synthesis

B. Gerard, R. Cencic, J. Pelletier,
J. A. Porco, Jr.* ―――――― **7831 – 7834**

Enantioselective Synthesis of the Complex Rocaglate (−)-Silvestrol

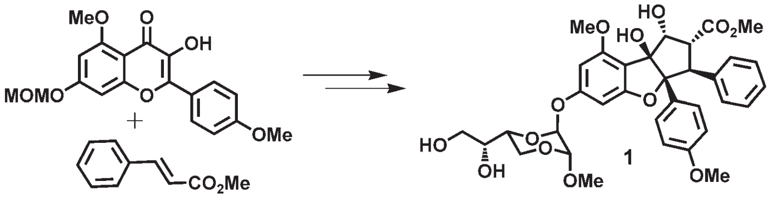

The total synthesis of the natural product (−)-silvestrol (**1**) has been accomplished and features enantioselective [3+2] photocycloaddition of a substituted 3-hydroxyflavone and methyl cinnamate promoted by a chiral Brønsted acid. Initial biological studies indicate a 5–10-fold greater activity of silvestrol as an inhibitor of protein synthesis in HeLa cells than its 1′′′′ diastereomer.

Natural Product Synthesis

M. El Sous, M. L. Khoo, G. Holloway,
D. Owen, P. J. Scammells,
M. A. Rizzacasa* ―――――― **7835 – 7838**

Total Synthesis of (−)-Episilvestrol and (−)-Silvestrol

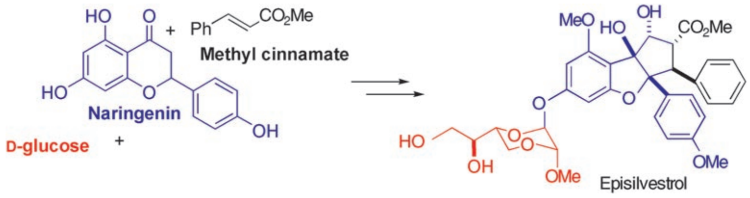

Sugar and spice... The total synthesis of the rare but potent anticancer natural product (−)-episilvestrol and its 5′′′ epimer (−)-silvestrol was accomplished from D-glucose, naringenin, and methyl cinnamate (see scheme). The key steps of the sequence were inspired by the possible biogenesis of these compounds.

Zeolite Analogues

E. A. Drylie, D. S. Wragg, E. R. Parnham,
P. S. Wheatley, A. M. Z. Slawin,
J. E. Warren, R. E. Morris* ― **7839 – 7843**

Ionothermal Synthesis of Unusual Choline-Templated Cobalt Aluminophosphates

Into the deep: A deep-eutectic solvent based on choline chloride and one of several carboxylic acids can be used to prepare cobalt aluminophosphate analogues of zeolites. One of the new materials contains unusual ring-opened double-four-ring units, in which a cobalt atom forms a terminal Co−Cl bond (see picture; Co cyan, Al gray, P purple, O red, Cl green).

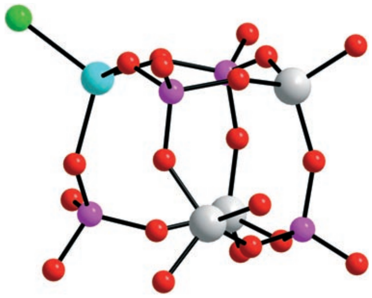

Cluster Compounds

S. K. Brayshaw, J. C. Green,* R. Edge,
E. J. L. McInnes, P. R. Raithby,*
J. E. Warren, A. S. Weller* ― **7844 – 7848**

$[Rh_7(PiPr_3)_6H_{18}][BAr^F_4]_2$: A Molecular Rh(111) Surface Decorated with 18 Hydrogen Atoms

Heptarhodium wagon wheel
$[Rh_7(PiPr_3)_6H_{18}][BAr^F_4]_2$ (shown), which resembles a planar Rh(111) surface with 18 hydride ligands, was obtained together with $[Rh_8(PiPr_3)_6H_{16}][BAr^F_4]_2$ from the reaction of $[Rh(PiPr_3)_2(nbd)][BAr^F_4]$ and $[Rh(nbd)_2][BAr^F_4]$ with hydrogen ($Ar^F = C_6H_3(CF_3)_2$, nbd = norbornadiene). Some of the H ligands are located in threefold hollows between Rh centers and thus mimic the orientation of atomic hydrogen adsorbed on Rh(111).

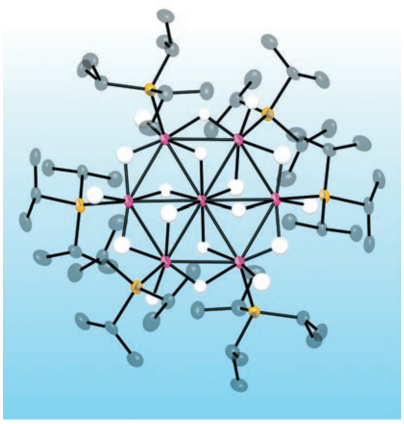

Getting turned on: An order-of-magnitude fluorescence amplification of simple tripodal sensors has been observed in the presence of phosphate ions. An X-ray structure analysis of one of the complexes (see picture) shows the binding of three phosphate ions, which closely resembles the anionic part of ATP, by the sensor. The sensors were used to generate cross-reactive arrays that can detect anions in human serum.

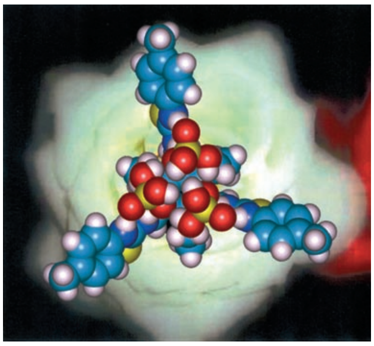

Analytical Methods

VIP

G. V. Zyryanov, M. A. Palacios,
P. Anzenbacher, Jr.* ———— **7849 – 7852**

Rational Design of a Fluorescence-Turn-On Sensor Array for Phosphates in Blood Serum

---

With or without the metal: Recently, the Grotthuss mechanism of proton transfer in water has been described in detail. A similar mechanism has been found in the vicinity of transition-metal ions, which leads to the formation of Zundel and Eigen complexes (see picture).

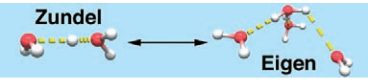

Ab Initio Calculations

O. Coskuner,* E. A. A. Jarvis,
T. C. Allison ———— **7853 – 7855**

Water Dissociation in the Presence of Metal Ions

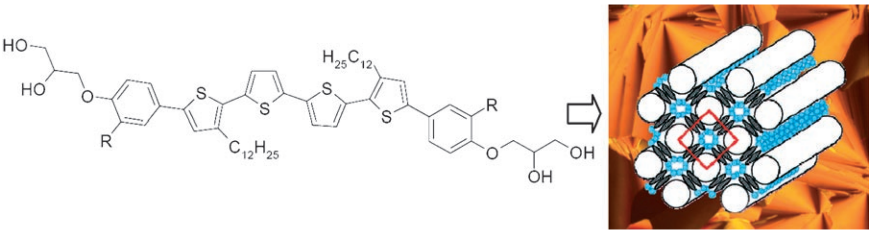

A good connection: A polyphilic oligothiophene derivative (see formula) forms a complex liquid-crystalline phase, in which the π-conjugated rods are organized in a honeycomb-like network of square cylinders (see picture). This arrangement opens new possibilities for the directed organization of π-conjugated organic materials into complex superstructures and patterns for the design of functional devices by means of liquid-crystal self-assembly.

Liquid Crystals

M. Prehm, G. Götz, P. Bäuerle, F. Liu,
X. Zeng, G. Ungar,
C. Tschierske* ———— **7856 – 7859**

Complex Liquid-Crystalline Superstructure of a π-Conjugated Oligothiophene

---

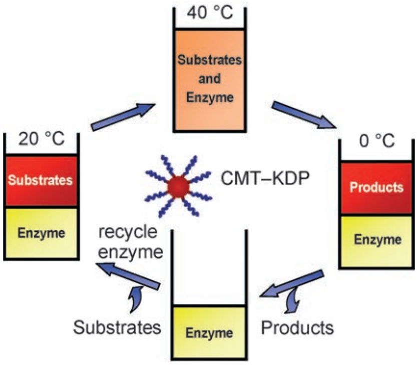

HIP to be green: Cytochrome *c* and α-chymotrypsin (CMT) can be solubilized in either fluorous solvents or supercritical CO_2 by hydrophobic ion pairing (HIP) with perfluorinated anionic surfactants (Krytox 157 FSL, KDP 4606). A model system for homogeneous fluorous biphasic biocatalysis involving the CMT–KDP complex in hexane/perfluoromethylcyclohexane is reported that simplifies both product separation and recycling of the biocatalyst.

Biphasic Biocatalysis

H. R. Hobbs, H. M. Kirke, M. Poliakoff,
N. R. Thomas* ———— **7860 – 7863**

Homogeneous Biocatalysis in both Fluorous Biphasic and Supercritical Carbon Dioxide Systems

Cluster Catalysis

J. Macht, M. J. Janik, M. Neurock,
E. Iglesia* ________ **7864 – 7868**

Catalytic Consequences of Composition in Polyoxometalate Clusters with Keggin Structure

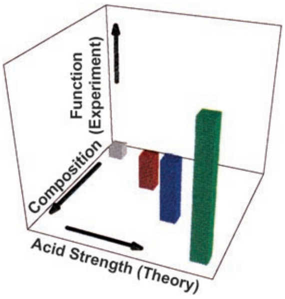

Rate constants for acid-catalyzed butanol dehydration on Keggin-type polyoxometalate clusters $H_{8-n}X^{n+}W_{12}O_{40}$ (X = P, Si, Al, Co) increase as the oxidation state of the central atom increases and the number of cluster protons concurrently decreases (see diagram). These trends reflect the lower deprotonation enthalpies of clusters with high valent central atoms and their stability as the anionic conjugate base in ionic transition states involved in dehydration catalysis.

Porphyrinoids

M. Stępień, L. Latos-Grażyński,*
N. Sprutta, P. Chwalisz,
L. Szterenberg ________ **7869 – 7873**

Expanded Porphyrin with a Split Personality: A Hückel–Möbius Aromaticity Switch

Dual identity: It takes a single phenylene twist to reveal the dichotomous nature of a di-*para*-benzihexaphyrin (see picture; phenylene rings highlighted in red). This expanded porphyrinoid switches between Hückel and Möbius topologies in an unusual solvent- and temperature-dependent equilibrium. Each of the two incarnations of the macrocycle has its own unmistakable spectral signature.

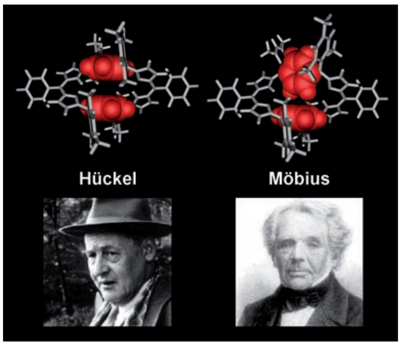

Surface Chemistry

D. Écija, R. Otero, L. Sánchez,
J. M. Gallego, Y. Wang, M. Alcamí,
F. Martín, N. Martín,*
R. Miranda* ________ **7874 – 7877**

Crossover Site-Selectivity in the Adsorption of the Fullerene Derivative PCBM on Au(111)

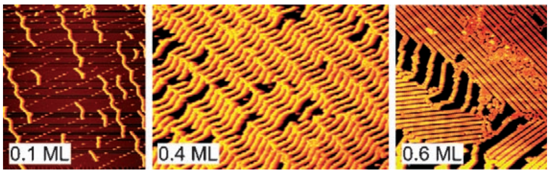

With increasing coverage, self-assembly of the fullerene derivative phenyl-C_{61}-butyric acid methyl ester (PCBM) on Au(111) undergoes a transition from substrate-controlled to hydrogen-bond-controlled. At low coverages, PCBM nucleates exclusively at the fcc areas of the “herringbone” reconstruction (left image). At higher coverages, double rows of PCBM molecules connected through hydrogen bonds are formed (right image). ML: monolayer.

C≡P Ligands

A. Ehlers,* J. G. Cordaro, D. Stein,
H. Grützmacher* ________ **7878 – 7881**

Mechanisms of Cyaphide (C≡P⁻) Formation

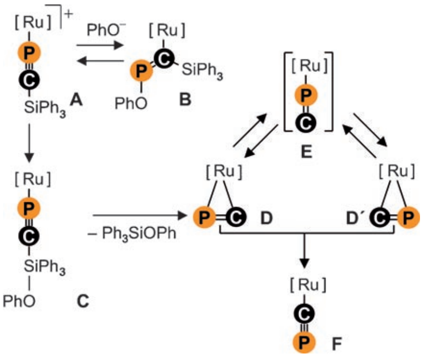

Rock ’n’ roll cyaphide: Although the kinetic product **B** is an observable intermediate of nucleophilic attack on the low-coordinate phosphorus atom in **A**, it is not directly involved in the mechanism leading to cyaphide complex **F**. Instead, DFT calculations suggest that nucleophilic attack at silicon (→**C**) initiates decomposition via **D** to **F**. In contrast to cyanide complexes, isocyaphide **E** is only a transition state for C≡P-ligand rotation **D**⇌**D′**.

Biosensors

F. Feng, Y. Tang, S. Wang,* Y. Li, D. Zhu ——— 7882 – 7886

Continuous Fluorometric Assays for Acetylcholinesterase Activity and Inhibition with Conjugated Polyelectrolytes

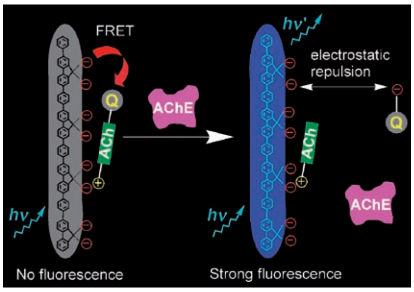

Quick but sensitive: A super-quenched fluorogenic complex of a cationic acetylcholine (ACh) derivative with an energy-acceptor tag and an anionic water-soluble conjugated polymer forms the basis of a highly effective fluorescence turn-on assay for studying the enzyme kinetics and inhibition of acetylcholinesterase (AChE; see schematic representation of the assay). FRET = fluorescence resonant energy transfer.

C–F Compounds

L. Hunter, A. M. Z. Slawin, P. Kirsch,* D. O'Hagan* ——— 7887 – 7890

Synthesis and Conformation of Multi-Vicinal Fluoroalkane Diastereoisomers

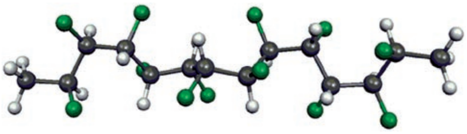

Doing the twist: Differences in behavior between isomers of straight-chain alkanes bearing four vicinal fluorine atoms are revealed by conformational analyses (X-ray diffraction, NMR spectroscopy). For example, computational studies show that the all-*syn* vicinal fluoroalkane (see picture, C gray, F green, H white) adopts a helical conformation, while the *anti*-*syn*-*anti* isomer prefers to be linear.

Surface Chemistry

K. T. Rim, M. Siaj, S. Xiao, M. Myers, V. D. Carpentier, L. Liu, C. Su, M. L. Steigerwald, M. S. Hybertsen, P. H. McBreen, G. W. Flynn,* C. Nuckolls* ——— 7891 – 7895

Forming Aromatic Hemispheres on Transition-Metal Surfaces

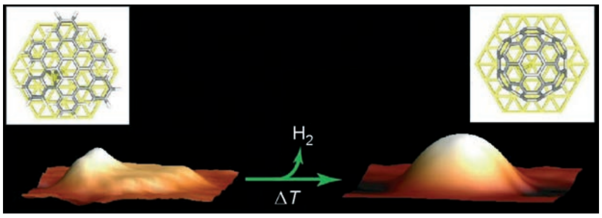

Bowled over: Hexabenzocoronene (HBC) binds to the surface of a ruthenium crystal through its "radialene" π bonds. Measurements on the product after heating of the HBC–surface complex are consistent with a bowl-shaped molecular fragment that is strongly bound, rim down, to the metal surface. This structure represents a new type of seed that could be used to grow single-walled carbon nanotubes of specific diameter and chirality.

Supporting information is available on the WWW (see article for access details).

A video clip is available as Supporting Information on the WWW (see article for access details).

The issues for October 2007 appeared online on the following dates
Issue 37: September 11. · Issue 38: September 17. · Issue 39: September 21. · Issue 40: September 28.

Service

Corrigendum

A DMSO-Compatible Orienting Medium: Towards the Investigation of the Stereochemistry of Natural Products

P. Haberz, J. Farjon,
C. Griesinger* ——— **427–429**

Angew. Chem. Int. Ed. **2005**, *44*

DOI 10.1002/anie.200461267

The authors would like to correct two points concerning their Communication. The first point affects the Supporting Information, in which there was a mix-up of assignments in the signals of menthol. This error is rectified in the Supporting Information that accompanies this Corrigendum. The authors point out that the fit of the theoretical and the experimental residual dipolar couplings improves.

The second point affects the Experimental Section: The preparation of the gels contained a neutralization step of the sulfonyl groups with NaOH. Insufficient washing thereafter of the mixture leads to gels that do not align. To avoid the preparation of such misaligned gels, a more precise experimental procedure is provided in the accompanying Supporting Information.

Corrigendum

Suzuki–Miyaura Coupling Reaction by Pd^{II}-Catalyzed Aromatic C–H Bond Activation Directed by an *N*-Alkyl Acetamino Group

Z. Shi,* B. Li, X. Wan, J. Cheng, Z. Fang,
B. Cao, C. Qin, Y. Wang ——— **5554–5558**

Angew. Chem. Int. Ed. **2007**, *46*

DOI 10.1002/anie.200700590

The principal address of the correspondence author and co-workers (except C.Q.) should be that at Beijing National Laboratory of Molecular Sciences (BNLMS) as listed second in this Communication. The fax number, email address, and homepage for the correspondence author are associated with this principal address. The authors apologize for this oversight.